ARCHIVES OF ACOUSTICS
29, 3, 447–459 (2004)

PHENOMENOLOGICAL MODEL OF CHANGES IN THE SPEED OF A SOUND WAVE IN CRYSTALS CAUSED BY DOPANTS

T. BŁACHOWICZ

Silesian University of Technology
Institute of Physics
Krzywoustego 2, 44-100 Gliwice, Poland
email: tblachow@zeus.polsl.gliwice.pl

(*received 21 December 2001; accepted 11 February 2004*)

The paper examines theoretically changes in the speed of an acoustic wave in crystals caused by metallic dopants. It is well known that an acoustic wave has a wavelength larger than the typical dimension of the elementary crystallographic cell, so it is sensitive only to large-scale features. The model bases on the assumption that a crystal with uniform distributed dopants can be transformed into a multiplayer virtual structure form which some conclusions can be drawn. The approach presented is valid for longitudinal acoustic waves, where the atomic displacement can be considered as a continuum field. It provides positive or negative changes in the acoustic wave speeds for different dopants in a hypothetical lithium niobate crystal.

Key words: Elastic constants, elastic waves in layered media, superlattices, lithium niobate, dopants in lithium niobate, Rytov's model, pulse-echo method, ultrasonics.

1. Introduction

Elasticity measurements of different type of materials can use acoustic waves from external sources, for example using the pulse-echo method [1] or they can take advantage of the use of natural Debye waves in light scattering experiments of Brillouin type [2–4]. In both methods, the acoustic wavelength is much larger that the dimension of a crystallographic cell. In other words, acoustic waves are sensitive only to large-scale features of the samples investigated. From the quantum point of view, acoustic phonons are sensitive to the large-scale features, while optic phonons are sensitive to local quantum effects at a sub-atomic scale.

Technical applications of doped crystals require the determination of the influence of the dopant concentration on the acoustic wave speeds, which are associated with the mechanical quality, or more precisely, with the disturbed crystallographic order during the technological treatment. This task requires also a proper theoretical background.

The relationships between the longitudinal wave speeds and the metallic dopant concentration examined here predict a speed decrease for some elements and an increase for others. It is assumed in the model that the elementary crystallographic cells posses a cubic symmetry and that the same symmetry is adopted by the elementary cell of the dopant material. The volume distribution of the dopants is uniform. The bulk volume of a real crystal is assumed to be build of virtual cubes of the same elementary volume and orientation. Inside of every cube an elementary cell of the dopant is localized, which dimensions are proportional to the dopant concentration. Because the provided symmetries are cubic, in the next step we can, transform this picture to a one-dimensional virtual periodical structure with an alternating layer of the basic substance and that of the dopant material. In this way we obtain a virtual superlattice. Next, from the weighted averaging procedure applied to a given doped superllatice, we can calculate the macroscopic quantity i.e the speed of the longitudinal acoustic wave. This is why the model can be called a Virtual Weighted Superlattice Model (VWSM) of doped crystals. Some features of the approach presented were adopted from the model introduced by RYTOV about 50 years ago [5].

Novel technological processes, those based mainly on the epitaxial growth, warrants preparation of artificial multilayered superlattices made of different metallic or semiconductor materials. More importantly, the elastic features measured can be compared with calculations based on the weighted averaging procedure. Good examples of these efforts can be found in the works of M. GRIMSDITCH [6]. Also, recent theoretical efforts of D. G. SEDRAKYAN and A. G. SEDRAKYAN for semiconductor superlattices with random thicknesses of layers [7] show the importance of the research field presented.

2. Assumptions of the Virtual Weighted Superlattice Model (VWSM)

The present model is narrowed to the long wavelength limit, to longitudinal acoustic waves and metal dopants of the same regular crystallographic lattice structure (Fe, Cu, Ag, Au, Al, Ta, Ni, V) and, most importantly, the model assumes that the uniform distribution of the dopant in a crystal can be thought of as a multilayered structure with a number of layers which dimensions are a function of the dopant concentration.

2.1. The Rytov's model of acoustic waves in superlattices

We take some advantage of the Rytov's model proposed about fifty years ago. It has been described partially in the two monographs [8, 9], mostly in relation to the application to semiconductors. Here, we try to remind it in the original form adopting however the results related mainly to the elasticity of superlattices built of two different solid state materials. Rytov considered also a multilayer consisting of a solid layer and a liquid layer, but these derivations are qualitatively similar to the solid-solid case. Nevertheless, the model seems nowadays still very useful due to the promising technological and industrial possibilities of multilayered systems.

The basic assumptions of the Rytov's model are as follows: it is related to a multilayered structure – an elementary bilayer can consist of two different solid sate materials or from a solid material and a liquid one. Next, it is valid for acoustic wavelengths much larger that the elementary bilayer thickness – it bases the solution of wave equations of motion with appropriate boundary conditions. Next, a multilayer is assumed to be isotropic in the plane of the layer, but in comparison to in-plane features it has a different behavior, into the direction parallel to the surface normal. Originally, the model provided the solution of the acoustic waves motion into the direction perpendicular to the sample surface. Figure 1 shows the coordinate system used in [5]. Rytov derived their formulas assuming hexagonal symmetry of the elementary cells of the materials. He derived five effective elastic constants for the multilayered superlattice.

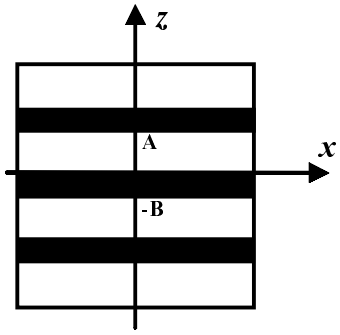

Fig. 1. The coordinate system of a multilayer in the Rytov's theory.

An arbitrary displacement the vector $\mathbf{U}$ of an infinitely small particle of the continuum medium can be splitted into rotational-less and source-less parts, $\mathbf{U} = \mathbf{w} + \mathbf{s}$, where $\mathrm{rot}\,\mathbf{w} = 0$, and $\mathrm{div}\,\mathbf{s} = 0$, respectively. This is why we can derive from a typical wave equation, with second spatial and temporal derivatives, the two following wave equations of motion related to both the parts mentioned

$$\begin{aligned} \frac{\partial^2 \mathbf{w}}{\partial t^2} - v_l^2 \mathrm{grad}\,\mathrm{div}\,\mathbf{w} = 0, \\ \frac{\partial^2 \mathbf{s}}{\partial t^2} - v_t^2 \mathrm{rot}\,\mathrm{rot}\,\mathbf{s} = 0, \end{aligned} \tag{1}$$

where v_l^2 and v_t^2 are the longitudinal and the transverse wave speeds expressed by an appropriate combination of the Lamé constants, λ and μ, namely

$$v_l^2 = (\lambda + 2\mu)/\rho \quad \text{and} \quad v_t^2 = \mu/\rho. \tag{2}$$

Then, narrowing our consideration to the $(z - x)$ saggital plane and assuming harmonic solutions of angular frequency ω, we obtain the following simplified wave equations

$$\begin{aligned} \frac{\partial^2 \mathbf{w}}{\partial t^2} + \frac{\partial^2 \mathbf{w}}{\partial z^2} + k_l^2 \mathbf{w} = 0, \qquad & \frac{\partial w_z}{\partial x} = \frac{\partial w_x}{\partial z} \quad (\text{rot}\,\mathbf{w} = 0)\,, \\ \frac{\partial^2 \mathbf{s}}{\partial t^2} + \frac{\partial^2 \mathbf{s}}{\partial z^2} + k_t^2 \mathbf{s} = 0, \qquad & \frac{\partial s_x}{\partial x} = -\frac{\partial s_z}{\partial z} \quad (\text{div}\,\mathbf{s} = 0)\,, \end{aligned} \tag{3}$$

where $k_l = \omega/v_l$ is the wave-vector value of the longitudinal wave and $k_t = \omega/v_t$ is the wave-vector value of the transverse wave.

A general solution of Eqs. (3) for a layer lying in the <0, A> range has following form

$$\begin{aligned} w_{xA} &= P_A(z)\,\exp[-ikx], & w_{zA} &= -\frac{1}{ik}\frac{dP_A(z)}{dz}\,\exp[-ikx], \\ s_{xA} &= \frac{1}{ik}\frac{dQ_A(z)}{dz}\,\exp[-ikx], & s_{zA} &= Q_A(z)\,\exp[-ikx], \end{aligned} \tag{4}$$

where k is the effective wave-vector value, the same for the whole multilayer, and $P_A(z)$ and $Q_A(z)$ are the following functions of k, the layer thickness A, and the wave-vectors k_{lA} and k_{tA} in this layer

$$P_A(z) = C_{1A}\cos\left[\sqrt{k_{lA}^2 - k^2}\;(z - A/2)\right] + C_{2A}\sin\left[\sqrt{k_{lA}^2 - k^2}\,(z - A/2)\right], \tag{5}$$

$$Q_A(z) = C_{3A}\cos\left[\sqrt{k_{tA}^2 - k^2}\;(z - A/2)\right] + C_{4A}\sin\left[\sqrt{k_{tA}^2 - k^2}\,(z - A/2)\right]. \tag{6}$$

This point of the derivation is very important because the first time the effective wave-vector $\mathbf{k}$, representing the whole multilayered structure, has been introduced. Similarly, solutions for the layer lying below the A layer (Fig. 1), in a range $< 0, -B >$, and marked by the B subscript, are equal to

$$\begin{aligned} w_{xB} &= P_B(z)\,\exp[-ikx], & w_{zB} &= -\frac{1}{ik}\frac{dP_B(z)}{dz}\,\exp[-ikx], \\ s_{xB} &= \frac{1}{ik}\frac{dQ_B(z)}{dz}\,\exp[-ikx], & s_{zB} &= Q_B(z)\,\exp[-ikx], \end{aligned} \tag{7}$$

with expressions for $P_B(z)$ and $Q_B(z)$ equal to

$$P_B(z) = C_{1B}\cos\left[\sqrt{k_{lB}^2 - k^2}\;(z + B/2)\right] + C_{2B}\sin\left[\sqrt{k_{lB}^2 - k^2}\,(z + B/2)\right], \tag{8}$$

$$Q_B(z) = C_{3B}\cos\left[\sqrt{k_{tB}^2 - k^2}\;(z + B/2)\right] + C_{4B}\sin\left[\sqrt{k_{tB}^2 - k^2}\,(z + B/2)\right]. \tag{9}$$

The solutions introduced above enable us to calculate the strain and stress tensor components. Then, appropriate continuity conditions at the interface between the layers and periodic conditions for the multilayered structure can be applied. Narrowing our considerations to longitudinal waves propagating along the surface normal, we have to

set the constants C_{2A}, C_{3A}, C_{2B}, C_{3B} equal to zero. For the transverse wave case the $C_{1A} = C_{4A} = C_{1B} = C_{4B} = 0$ condition should be fulfilled.

At the interface between the two types of materials, where $z = 0$, the continuity conditions have the following form

$$\begin{aligned} U_{x(A)}(0) &= U_{x(B)}(0), \qquad U_{z(A)}(0) = U_{z(B)}(0), \\ T_{xz(A)}(0) &= T_{xz(B)}(0), \qquad T_{zz(A)}(0) = T_{zz(B)}(0). \end{aligned} \tag{10}$$

Appropriate periodicity conditions, valid for the $z = A$ and $z = -B$ coordinates, are as follows

$$\begin{aligned} U_{x(A)}(A) &= U_{x(B)}(-B), \qquad U_{z(A)}(A) = U_{z(B)}(-B), \\ T_{xz(A)}(A) &= T_{xz(B)}(-B), \qquad T_{zz(A)}(A) = T_{zz(B)}(-B), \end{aligned} \tag{11}$$

where both in (10) and in (11) the strain tensor components, T_{ij} (i, j, = x or z), can be calculated applying Lamé constants and using the following definitions for the strain and stress tensors

$$T_{ij} = \lambda S_{ik}\delta_{ik} + 2\mu S_{ik}, \tag{12}$$

and

$$S_{ik} = \frac{1}{2}\left(\frac{\partial U_i}{\partial x_k} + \frac{\partial U_k}{\partial x_i}\right), \tag{13}$$

respectively, where δ_{ik} is the Kronecker's delta.

As was mentioned above, the $C_{2A} = C_{3A} = C_{2B} = C_{3B} = 0$ condition, valid for longitudinal waves, along with the boundary and periodic conditions (10) and (11) and with the solutions given by the formulas (4)–(9) results in a (4×4)-dimension determinant, which value equal to zero provide a unique solution of the problem and a dispersion relation, that is a relation between the frequency and the wave vector for the longitudinal wave $\omega = v_l k$, where v_l is the speed of the longitudinal acoustic wave in the whole structure. The dispersion relation, derived from the determinant, can be written in the following manner

$$\begin{aligned} &4\left(\mu_A - \mu_B\right)^2 X_A X_B + \omega^2\rho_A\left[\frac{\omega^2\rho_A}{k^2} - 4\left(\mu_A - \mu_B\right)\right] X_B \tan\left(\frac{\sqrt{k_{tA}^2 - k^2}A}{2}\right) \\ &\qquad + \omega^2\rho_B\left[\frac{\omega^2\rho_B}{k^2} + 4\left(\mu_A - \mu_B\right)\right] X_A \tan\left(\frac{\sqrt{k_{tB}^2 - k^2}B}{2}\right) \\ &- \frac{\omega^4\rho_A\rho_B}{k^2}\left(Y_A \tan\left(\frac{\sqrt{k_{tB}^2 - k^2}B}{2}\right) + Y_B \tan\left(\frac{\sqrt{k_{tA}^2 - k^2}A}{2}\right)\right) = 0, \end{aligned} \tag{14}$$

where the expressions for X_A, X_B, Y_A, Y_B, related to the A and B layers, are given by

$$\begin{aligned}
X_A &= k^2\tan\left(\frac{\sqrt{k_{tA}^2-k^2}A}{2}\right)+\sqrt{k_{lA}^2-k^2}\sqrt{k_{tA}^2-k^2}\tan\left(\frac{\sqrt{k_{lA}^2-k^2}A}{2}\right),\\
X_B &= k^2\tan\left(\frac{\sqrt{k_{tB}^2-k^2}B}{2}\right)+\sqrt{k_{lB}^2-k^2}\sqrt{k_{tB}^2-k^2}\tan\left(\frac{\sqrt{k_{lB}^2-k^2}B}{2}\right),\\
Y_A &= k^2\tan\left(\frac{\sqrt{k_{tA}^2-k^2}A}{2}\right)-\sqrt{k_{lB}^2-k^2}\sqrt{k_{tA}^2-k^2}\tan\left(\frac{\sqrt{k_{lB}^2-k^2}B}{2}\right),\\
Y_B &= k^2\tan\left(\frac{\sqrt{k_{tB}^2-k^2}B}{2}\right)-\sqrt{k_{lA}^2-k^2}\sqrt{k_{tB}^2-k^2}\tan\left(\frac{\sqrt{k_{lA}^2-k^2}A}{2}\right).
\end{aligned} \tag{15}$$

Rytov derived finally his formulas in a long wavelength limit, which means a transformation from all the above tangent functions into its arguments. Next, from Eq. (14) the longitudinal acoustic wave speed v_l can be calculated. Finally, the formulas for the v_l, and the effective density ρ of the sample as a whole provided below, possess a mathematical character of weighted averages, namely

$$v_l^2=\frac{1+4w_Aw_B\left(\mu_A-\mu_B\right)\left(\lambda_A-\lambda_B+\mu_A-\mu_B\right)}{\rho[w_A\left(\lambda_B+2\mu_B\right)+w_B\left(\lambda_A+2\mu_A\right)]}, \tag{16}$$

where the expressions

$$w_A=\frac{A}{A+B}\quad\text{and}\quad w_B=\frac{B}{A+B} \tag{17}$$

work as the weights. The effective density of the medium is a simple average calculated from densities of the constituents, ρ_A and ρ_B, and is equal to

$$\rho=w_A\rho_A+w_B\rho_B. \tag{18}$$

The introduction of effective parameters for the multilayered structure as a whole: the elastic constants, the density, and the wave-vector is the original Rytov's contribution to the elasticity of multilayered structures.

Now, we switch our attention to a more disordered system, to a doped crystal, and we try to take advantage of the Rytov's averaging approach. We try to prove that such a system can be equivalent, to some degree, to a multilayered superlattice.

2.2. Calculation of the effective longitudinal acoustic wave speed in a multilayered structure

The main ideas of the approach proposed here were described briefly in the Introduction. The main spatial period of the virtual one-dimensional structure consists of

two layers; the first one being made of a pure crystal material and the second one created from the dopant material (Fig. 2). The value of the main one-dimensional period is assumed to be calculated from the dopant volume concentration n_2 and is equal to

$$d = (n_2)^{-1/3}\,. \tag{19}$$

The quantity d measures the elementary length, where the two substances are placed in an artificial periodical way. Because the number of dopant atoms is less than that of the atoms of pure crystal, it seems natural to take the concentration of the dopant as the d quantity. This determines the one-dimensional virtual space to be filled by both substances: the pure material and the metallic dopant.

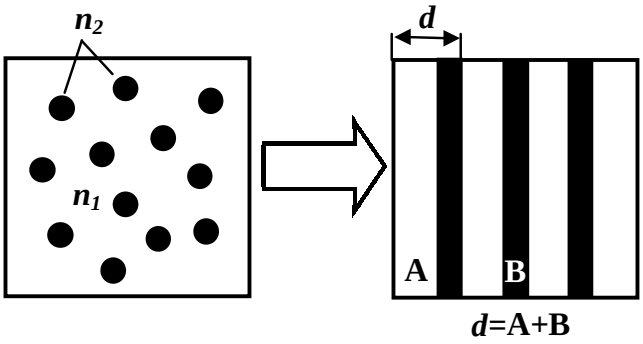

Fig. 2. The transformation procedure from uniform distributed dopants of concentration n_2 to artificial multilayered structures. Descriptions: d is the double layer thickness, A is the $LiNbO_3$ layer thickness, B is the dopant thickness, and n_1 represents the concentration the $LiNbO_3$ molecules after doping.

Next, the ratio of thickness for the 2-layered pure-material/dopant system is equal to

$$\frac{A}{B} = \left(\frac{n_0 - n_2}{n_2}\right)^{1/3}, \tag{20}$$

where A is the thickness of the layer related to the pure crystal material, B is the thickness of the layer related to the dopant layer, n_0 is the concentration of molecules in the pure crystal, and n_2 is the volume dopant concentration. In Eq. (20) it is assumed that the total volume crystal is constant or, in other words, that some pure crystal molecules were substituted by dopand atoms $-\,n_1 = n_0 - n_2$. Following the obvious relation $d = A + B$, and using Eqs. (19)–(20), we can derive formulas for the A and B thicknesses as functions of the concentration of pure crystal molecules and the dopant concentration

$$A = d\frac{(n_0 - n_2)^{1/3}}{n_2^{1/3} + (n_0 - n_2)^{1/3}}, \tag{21}$$

and

$$B = d\frac{n_2^{1/3}}{n_2^{1/3} + (n_0 - n_2)^{1/3}}. \tag{22}$$

It will be proved now that this bilayered system possesses all information related to the whole multilayered structure. The same feature possesses the Rytov's model thanks to its periodical conditions (11).

By solving the dispersion relation (14) and making use of the boundary conditions (10)–(11), one obtains the following dispersion relation for a longitudinal acoustic wave

$$\cos(kd) = \cos\left[\omega\left(\frac{A}{v_{lA}} + \frac{B}{v_{lB}}\right)\right] - \frac{\varepsilon^2}{2}\sin\left(\omega\frac{A}{v_{lA}}\right)\sin\left(\omega\frac{B}{v_{lB}}\right), \tag{23}$$

where k is the resulting wavevector for both the layers, v_{lA} is the speed of the wave in the first layer, v_{lB} the same speed in the second one, and ε is the mismatch of impedances expressed by the following equation

$$\varepsilon = \frac{v_{lA}\rho_A - v_{lB}\rho_B}{v_{lA}\rho_A + v_{lB}\rho_B}. \tag{24}$$

G. P. SRIVASTAVA [9] showed the limit for Eq. (24), for long wavelengths, when $k \to 0$ and $\omega \to 0$, and when the above equation reduces to $\omega = kv_l$, that means, to the simple relation with the effective longitudinal acoustic wave speed v_l equal to

$$v_l = \frac{A+B}{\sqrt{\left(\frac{A}{v_{lA}} + \frac{B}{v_{lB}}\right)^2 - \varepsilon^2\frac{A}{v_{lA}}\cdot\frac{B}{v_{lB}}}}. \tag{25}$$

As mentioned above, the average acoustic wave speed is identical for both layers.

Now, it will be shown that the average speed does not depend on the number of layers in a multilayered structure. By expanding Eq. (25) into an N double-layered system, one obtains

$$\begin{aligned} v_l &= \frac{A^{(1)} + B^{(1)} + \cdots + A^{(N)} + B^{(N)}}{\sqrt{\left(\frac{A^{(1)}}{v_{lA}^{(1)}} + \frac{B^{(1)}}{v_{lB}^{(1)}} + \cdots + \frac{A^{(N)}}{v_{lA}^{(\mathrm{N})}} + \frac{B^{(N)}}{v_{lB}^{(\mathrm{N})}}\right)^2}} \\ &\qquad \frac{A^{(1)} + B^{(1)} + \cdots + A^{(N)} + B^{(N)}}{-\varepsilon^2\left(\frac{A^{(1)}}{v_{lA}^{(1)}} \times \frac{B^{(1)}}{v_{lB}^{(1)}} \times \cdots \times \frac{A^{(N)}}{v_{lA}^{(\mathrm{N})}} \times \frac{B^{(N)}}{v_{lB}^{(\mathrm{N})}}\right)} \\ &= \frac{NA + NB}{\sqrt{N^2 \times \left(\frac{A}{v_{lA}} + \frac{B}{v_{lB}}\right)^2 - \varepsilon^2 \times \left(\frac{A}{v_{lA}} \times \frac{B}{v_{lB}}\right)^N}} \cong \frac{A+B}{\frac{A}{v_{lA}} + \frac{B}{v_{lB}}}, \end{aligned} \tag{26}$$

where to a very good approximation the second term in the denominator can be omitted.

2.3. Numerical results of calculations

For numerical calculations the following metals were chosen: Fe, Cu, Ag, Au, Al, Ta, Ni, and V. The values of their elastic constants (c_{11}), and densities collected from different papers can be found in N. W. ASHCROFT's and N. D. MERMIN's monograph [10]. The range of the dopant concentration applied here is equal to (10^9 m^{-3} – 10^{26} m^{-3}). The natural concentration of molecules in the pure $LiNbO_3$ crystal, taken for calculations, is equal to about 10^{28} m^{-3}. The calculations do not take into account the influence of the piezoelectric effect, i.e. in that sense the calculations are approximate.

The results of calculations are given in Tables 1–3. Table 1 provides information about the dimensions of the virtual layers. The last column gives values of the A/B ratio, showing how the model works. Table 2 gives the aforementioned impedance mismatch. Most of its values are negative, for aluminum the value is positive. Table 3 gives the values of the average speed as a function of the dopant concentration. The results of these dependencies are presented in Fig. 3. For convenience, three types of scales of the dopant concentrations are shown. For concentrations of the 10^{19} m^{-3} order, the changes in the speed of the acoustic wave, are on the 2–4 m/s level. For higher concentrations, up to 10^{26} m^{-3}, they are equal to 400–600 m/s. However, it seems that such higher concentrations have no technological importance. The most relevant result is that the model predicts a positive change in the speeds for the Al and Fe doping, and negative changes for the rest of the metals.

Table 1. Dimensions of multilayered structures for different dopant concentrations.

Dopant concentration n_2 [m^{-3}]	Double layer thickness d [m]	Number of layers N	$LiNbO_3$ layer thickness A [m]	Metal layer thickness B [m]	Ratio of layers thickness A/B
10^{9}	1.00×10^{-03}	10	1.00×10^{-03}	3.75550×10^{-10}	2662761.93
10^{10}	4.64×10^{-04}	21	4.64×10^{-04}	3.75550×10^{-10}	1235944.60
10^{11}	2.15×10^{-04}	46	2.15×10^{-04}	3.75549×10^{-10}	573674.67
10^{12}	1.00×10^{-04}	100	1.00×10^{-04}	3.75548×10^{-10}	266276.19
10^{13}	4.64×10^{-05}	215	4.64×10^{-05}	3.75547×10^{-10}	123594.46
10^{14}	2.15×10^{-05}	464	2.15×10^{-05}	3.75543×10^{-10}	57367.47
10^{15}	1.00×10^{-05}	1000	1.00×10^{-05}	3.75536×10^{-10}	26627.62
10^{16}	4.64×10^{-06}	2154	4.64×10^{-06}	3.75520×10^{-10}	12359.45
10^{17}	2.15×10^{-06}	4641	2.15×10^{-06}	3.75484×10^{-10}	5736.75
10^{18}	1.00×10^{-06}	10000	1.00×10^{-06}	3.75409×10^{-10}	2662.76
10^{19}	4.64×10^{-07}	21544	4.64×10^{-07}	3.75246×10^{-10}	1235.94
10^{20}	2.15×10^{-07}	46415	2.15×10^{-07}	3.74896×10^{-10}	573.67
10^{21}	1.00×10^{-07}	100000	9.96×10^{-08}	3.74145×10^{-10}	266.28
10^{22}	4.64×10^{-08}	215443	4.60×10^{-08}	3.72536×10^{-10}	123.59
10^{23}	2.15×10^{-08}	464158	2.12×10^{-08}	3.69116×10^{-10}	57.37
10^{24}	1.00×10^{-08}	1000000	9.64×10^{-09}	3.61963×10^{-10}	26.63
10^{25}	4.64×10^{-09}	2154434	4.29×10^{-09}	3.47495×10^{-10}	12.36
10^{26}	2.15×10^{-09}	4641588	1.83×10^{-09}	3.20286×10^{-10}	5.73

Table 2. Impedance mismatch and speed of the longitudinal acoustic wave for different materials.

Metal elements	The c_{11} elastic constant [Pa] x 10^{11}	Density [kg/m^3]	Impedance mismatch	Speed in the pure material [m/s]
Fe	2.34	7900	-0.97941	5442.45
Cu	1.68	8800	-0.22577	4369.31
Ag	1.24	10500	-0.39425	3436.50
Au	1.86	19296	-0.58708	3104.72
Al	1.07	2700	0.69054	6295.21
Ta	2.67	16600	-0.65196	4010.53
Ni	2.45	8800	-0.39556	5276.45
V	2.29	5960	-0.18752	6198.61
$LiNbO_3$	2.01	4640		6585.81

Table 3. Speed of the longitudinal acoustic wave in the doped $LiNbO_3$ crystal for different amounts of concentration. The dopants: Fe, Cu, Ag, Au, Al, Ta, Ni, and V.

Dopant concentration n_2 [m^{-3}]	Speed of wave-Fe [m/s]	Speed of wave-Cu [m/s]	Speed of wave-Ag [m/s]	Speed of wave-Au [m/s]	Speed of wave-Al [m/s]	Speed of wave-Ta [m/s]	Speed of wave-Ni [m/s]	Speed of wave-V [m/s]
10^{9}	6585.81	6585.81	6585.80	6585.80	6585.81	6585.81	6585.81	6585.81
10^{10}	6585.81	6585.80	6585.80	6585.80	6585.81	6585.80	6585.81	6585.81
10^{11}	6585.81	6585.80	6585.80	6585.80	6585.81	6585.80	6585.80	6585.81
10^{12}	6585.82	6585.79	6585.79	6585.79	6585.81	6585.80	6585.80	6585.80
10^{13}	6585.83	6585.78	6585.77	6585.77	6585.82	6585.79	6585.80	6585.80
10^{14}	6585.85	6585.75	6585.72	6585.72	6585.83	6585.77	6585.79	6585.80
10^{15}	6585.90	6585.69	6585.62	6585.62	6585.86	6585.73	6585.77	6585.79
10^{16}	6586.00	6585.56	6585.40	6585.40	6585.91	6585.65	6585.73	6585.78
10^{17}	6586.23	6585.27	6584.93	6584.94	6586.04	6585.47	6585.63	6585.76
10^{18}	6586.71	6584.65	6583.91	6583.94	6586.31	6585.08	6585.43	6585.70
10^{19}	6587.75	6583.31	6581.72	6581.78	6586.89	6584.24	6585.00	6585.57
10^{20}	6589.98	6580.44	6577.02	6577.14	6588.13	6582.44	6584.08	6585.30
10^{21}	6594.77	6574.27	6566.92	6567.17	6590.80	6578.54	6582.09	6584.73
10^{22}	6604.94	6561.09	6545.37	6545.81	6596.47	6570.13	6577.81	6583.48
10^{23}	6626.23	6533.22	6499.82	6500.31	6608.37	6551.92	6568.64	6580.83
10^{24}	6669.28	6475.43	6405.62	6404.83	6632.59	6512.38	6549.13	6575.22
10^{25}	6749.81	6360.57	6219.41	6211.11	6678.71	6426.74	6508.25	6563.57
10^{26}	6874.61	6149.88	5882.67	5847.13	6754.64	6246.20	6425.79	6540.41

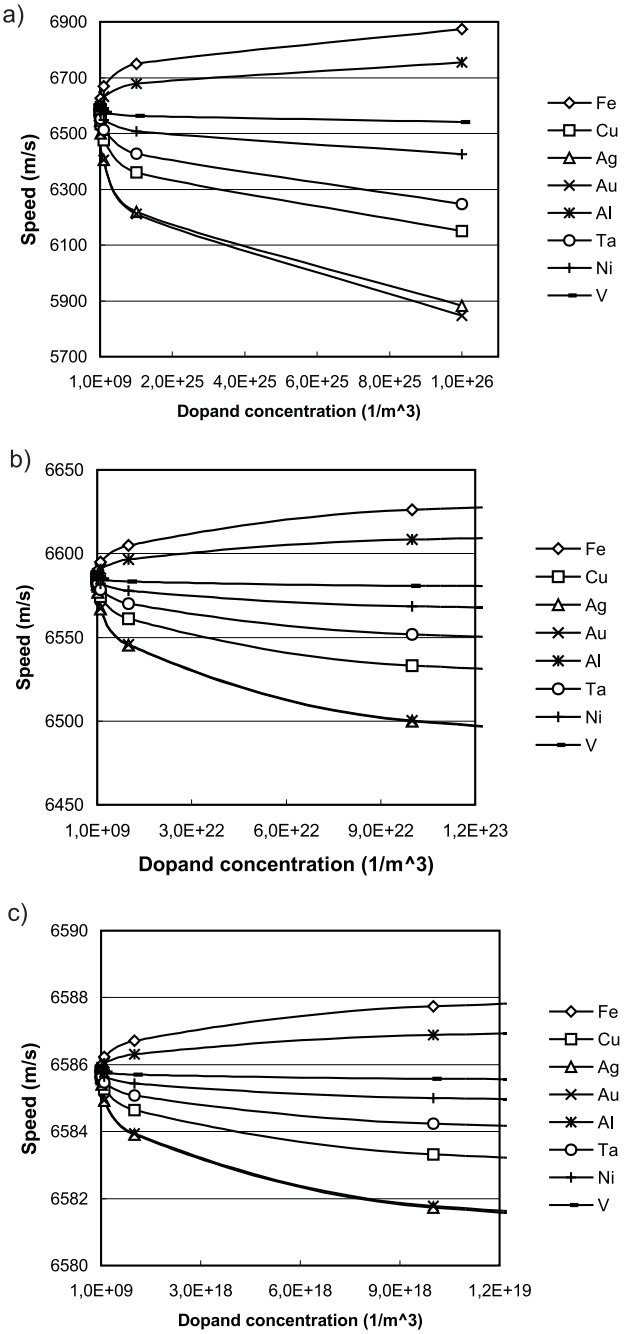

Fig. 3. Changes in the speed of an acoustic wave as function of dopant concentrations for different scales; the 10^9 m^{-3} to 10^{26} m^{-3} range (a), the 10^9 m^{-3} to 10^{23} m^{-3} range (b), and the 10^9 m^{-3} to 10^{19} m^{-3} range (c).

3. Conclusions

The proposed 1-dimensional model for longitudinal acoustic waves describes changes of their speed as a function of the dopant concentration. For dopant concentrations larger than 10^{24} m^{-3}, the dependencies of the speed changes are quasi-linear, while for smaller concentrations they are nonlinear.

From the technological point of view, where the dopant concentrations are relatively not so high, an appropriate method of verification of the provided theory should be based on a precise ultrasonic method, for example the pulse-echo method in which an accuracy of 0.1 m/s in ultrasonic speed measurements can be easily achieved [11].

In the model presented, we have tried to formalize the influence of the doping process on the acoustical properties of crystals. The doping rely on the adding of some atoms, for example of the order of 10^{-2} mol% [12], which means in practice that one atom of the dopant is placed very rarely between the basic material atoms. The acoustic wave is an ideal object to test such features because a typical acoustic wave of a frequency of 10 MHz, encompasses about 10^6 elementary crystallographic lattice constants. On the other hand, the wave is not sensitive to very local disturbances in the dopants concentration, even if such disturbances take place. This is why in the long wavelength limit, in the sense presented by the Rytov's approach, the introduced one-dimensional virtual superlattice is legitimate and enabled us to perform the calculation of changes in the speed of an acoustic wave in crystals caused by dopants.

References

[1] PAPADAKIS E. P., *Ultrasonic attenuation and speed in three transformation products in steel*, J. Appl. Phys., **35**, 1474–1482 (1964).

[2] BŁACHOWICZ T., *On the scattering of light on sound waves in the hypersonic range of frequencies; II. The directional sensitivity of Brillouin light scattering*, Central European Journal of Physics, CEJP **1**, 153–178 (2003), available on-line at http://www.cesj.com/physics.html.

[3] BŁACHOWICZ T., *Study of the elastic properties of the lithium tantalate crystal by the Brillouin light scattering*, Archives of Acoustics, **25**, 23–34 (2000).

[4] BŁACHOWICZ T., *Numerical calculations of the rotational contributions to a scattering coefficient in the piezoelectric $LiTaO_3$ crystal*, J. Opt. Soc. Am., **B15**, 2599–2606 (1998).

[5] RYTOV S. M., *Akustitscheskie svojjstva mellkosloistnojj sredy*, Akust. Zurn., **2**, 71–83 (1956).

[6] GRIMSDITCH M., [in:] *Light scattering in solids*, V, M. Cardona and G. Güntherodt, [Eds.], Springer-Verlag, p.285, Berlin, Heildelberg, New York 1989.

[7] SEDRAKYAN D. G., SEDRAKYAN A. G., *Localization of phonons in two component superlattice with random thicknesses of the layers*, arXiv:cond-mat/9810329 preprint, 24 Oct. 1998.

[8] JUSSERAND B., [in:] *Light scattering in solids*, V, M. Cardona and G. Güntherodt, [Eds.], Springer-Verlag, p.49, Berlin, Heildelberg, New York 1989.

[9] SRIVASTAVA G. P., *The physics of phonons*, Adam Hilger, 264–267, Bristol 1990.

[10] ASHCROFT N. W., MERMIN N. D., *Solid state physics*, Holt-Rinehart-Winston 1976.

[11] BŁACHOWICZ T., KLESZCZEWSKI Z., SKUMIEL A., *Elastic constants of the $SrLaAlO_4$ and $SrLaGaO_4$ crystals measured for ultrasonic and hypersonic acoustic frequencies*, Ultrasonics, **39**, 611–615 (2002).

[12] BŁACHOWICZ T., PYKA M., KLESZCZEWSKI Z., ŚWIRKOWICZ M., ŁUKASIEWICZ T., *Doping effects of Cu ions on the elastic properties of the $LiNbO_3$ crystal uncovered by Brillouin scattering*, Sol. Stat. Comm., **123**, 317–319 (2002).